Computers & Geosciences 35 (2009) 1897–1906

Contents lists available at ScienceDirect

Computers & Geosciences

journal homepage: www.elsevier.com/locate/cageo

Coupling geological and numerical models to simulate groundwater flow and contaminant transport in fractured media

Daniela Blessent [a,*], René Therrien [a], Kerry MacQuarrie [b]

[a] Département de Géologie et Génie Géologique, Université Laval, Ste-Foy, Québec, Canada G1K 7P4
[b] Department of Civil Engineering, University of New Brunswick, P.O. Box 4400, Fredericton, New Brunswick, Canada E3B 5A3

ARTICLE INFO

Article history:
Received 22 May 2008
Received in revised form
12 December 2008
Accepted 13 December 2008

Keywords:
Numerical modeling
Fractures
Geomodel
Tetrahedra
Influence coefficient technique

ABSTRACT

A new modeling approach is presented to improve numerical simulations of groundwater flow and contaminant transport in fractured geological media. The approach couples geological and numerical models through an intermediate mesh generation phase. As a first step, a platform for 3D geological modeling is used to represent fractures as 2D surfaces with arbitrary shape and orientation in 3D space. The advantage of the geological modeling platform is that 2D triangulated fracture surfaces are modeled and visualized before building a 3D mesh. The triangulated fractures are then transferred to the mesh generation software that discretizes the 3D simulation domain with tetrahedral elements. The 2D triangular fracture elements do not cut through the 3D tetrahedral elements, but they rather form interfaces with them. The tetrahedral mesh is then used for 3D groundwater flow and contaminant transport simulations in discretely fractured porous media. The resulting mesh for the 2D fractures and 3D rock matrix is checked to ensure that there are no negative transmissibilities in the discretized flow and transport equation, to avoid unrealistic results. To test the validity of the approach, flow and transport simulations for a tetrahedral mesh are compared to simulations using a block-based mesh and with results of an analytical solution. The fluid conductance matrix for the tetrahedral mesh is also analyzed and compared with known matrix values.

1. Introduction

The simulation of groundwater flow and contaminant transport in geological formations requires three steps: (1) characterizing the geology and developing conceptual models of the hydrogeology and hydrologic material properties, (2) building the computational grid and prescribing initial and boundary conditions and (3) applying numerical models for fluid flow, energy transport, and/or chemical transport (Gable et al., 1996b). Because of the capabilities of CAD systems to represent and visualize complex 3D geological objects, such as fractures, CAD systems and hydrogeological models have been increasingly combined to study fractured rocks. From a hydrogeological point of view, fractured rocks are complex and are characterized by a porous rock mass dissected by various types of discontinuities, which are referred to as fractures. The rock mass typically has a low permeability and high storage capacity, while hydraulically active fractures have high permeability but lower storage capacity because of their lower contribution to the total porosity of the rock mass. Because they are permeable, fractures can therefore be preferential pathways for contaminants. Transport processes in fractured rocks include molecular diffusion, mechanical dispersion and advection. In the rock matrix, molecular diffusion usually dominates over advection, such that the porous rock mass may attenuate and retard the advective propagation of contaminants along fractures (Tang et al., 1981; Therrien and Sudicky, 1996). Representation of all fluid flow and transport processes is required to realistically simulate the hydrogeological behavior of fractured rocks. Depending on the scale of investigation and on the fracture properties, two main conceptual models exist to represent fractured media: the equivalent continuum model, where fractures in the rock mass are not explicitly discretized, and the discrete fracture model, where fractures are discretized. This investigation addresses the discrete fracture representation and focuses on the discretization of individual fractures.

The 3D geometrical representation of subsurface geological structures, including fractures, is called the geological model, or the Geomodel (Mallet, 2002). A mesh generation phase, representing the connection between the geological and the numerical models, is necessary to discretize the Geomodel. The key problem to solve here is this connection, and the challenge is to understand the tradeoff between a high-resolution model that represents hydrostratigraphy with a high degree of fidelity and a lower resolution model that is perhaps better suited for intensive

* Corresponding author. Tel.: +1 418 934 7574.
E-mail address: daniela.blessent.1@ulaval.ca (D. Blessent).

0098-3004/$ - see front matter © 2009 Elsevier Ltd. All rights reserved.
doi:10.1016/j.cageo.2008.12.008

Nomenclature

$2b$	fracture aperture (L)
A	fluid conductance matrix
c	solute concentration (ML^{-3})
D_0	free-solution diffusion coefficient (L^2T^{-1})
D_{ij}	hydrodynamic dispersion coefficient (L^2T^{-1})
F_{ij}	Voronoi cell face area (L^2)
K_{ij}	saturated hydraulic conductivity tensor (LT^{-1})
N	finite element basis function
R	retardation factor
S_s	specific storage (L^{-1})
V	tetrahedron volume (L^3)
v	velocity of groundwater flow (LT^{-1})
α_L	longitudinal dispersivity (L)
η_i	set of nodes connected to node i
λ	solute decay constant (T^{-1})

computations (Bower et al., 2005). Some studies have already been conducted to couple a Geomodel with a numerical code to simulate physical phenomena.

Kalbacher et al. (2005) proposed an interface between the GOCAD platform[1] and the numerical software Rockflow (Kolditz and Bauer, 2004; Kolditz et al., 2008). They considered a 2.5D fractured rock network, consisting of just planar surfaces in the 3D space, and represented the network as a triangular mesh in GOCAD. They did not discretize the rock matrix and only used 2D triangular finite elements. They used the GMSH meshing software[2] to generate a suitable mesh for the numerical model. They noted that generating and transforming the mesh within GOCAD can lead to numerical errors during mesh generation or when using other features of the CAD. These errors are difficult to locate and it is difficult to correct or remove them once the mesh is generated (Kalbacher et al., 2005).

Andenmatten-Berthoud and Kohl (2003) discretized a complex geological site that contains faults by using the TGridlab GOCAD plug-in, which generates a tetrahedral mesh. TGridlab is applicable if the domain can be represented as an assemblage of surface boundaries that define closed volumes. Surface boundaries can be fractures, fault surfaces or the boundary of the geological domain. Once the domain boundary has been represented, the 3D domain is discretized with tetrahedra, using the TGridlab plug-in. The discretization is complicated if there are complex fault configurations or fracture intersections and it becomes impossible if the 3D boundary representation does not describe closed volumes.

Taniguchi and Fillion (1996) applied an approach similar to that of Andenmatten-Berthoud and Kohl (2003). They divided the whole fractured geological domain into subdomains separated by fracture planes. They triangulated each subdomain independently into tetrahedra, which are further subdivided into hexahedra.

A new approach for discretizing arbitrary fracture networks embedded into a porous rock matrix is introduced here. The discretization of the rock matrix is necessary for contaminant transport simulations where matrix diffusion is significant. Discretization therefore requires a simultaneous generation of 3D and 2D elements to represent, respectively, the rock matrix and the fractures. In the general case, fractures can have any orientation in space, they may be non-planar, and may intersect. Additionally, fractures might not extend to the external domain boundaries, making it impossible to create 3D volumetric regions bounded by fracture surfaces as required by previous studies. As a result, the discretization approach must represent triangulated fractures embedded in a 3D tetrahedral mesh representing the surrounding rock matrix. A key requirement of the approach proposed here is to ensure that tetrahedra fit exactly the fracture surface patterns, such that a tetrahedral face matches a triangle belonging to a fracture surface. The novelty of the approach is that it takes advantage of a geological modeling platform to represent fractures and combines a CAD system and a hydrogeological numerical model to improve modeling capabilities.

2. Geological model and mesh generation

A CAD system is designed for precise editing and management of spatial data and is therefore well suited for hydrogeological models that require well-defined and well-located spatial data. To represent fractured geological formations, the discretely fractured conceptual model is chosen here and fracture zones have to be explicitly represented. Because subsurface geological structures are neither directly accessible nor fully known, the Geomodel is built from local and scattered data obtained from field investigations. The data must be interpolated to create a 3D representation of the subsurface. A geological modeling platform, such as GOCAD, can efficiently interpolate 3D spatial data. This software is based on an interpolation method for modeling natural objects and representing a wide variety of complex data. As opposed to traditional CAD systems that simply create attractive geometrical entities without any constraints, GOCAD has been designed to generate more complex structures and take into account the physical properties attached to each object.

The Geomodel is then discretized with the LaGriT software,[3] which has been developed at the Los Alamos National Laboratory. Among possible mesh generators investigated, LaGriT has been chosen because it offers the greatest number of advantages. Mesh generation is a key link between Geomodels and numerical models. Mesh generation must capture complex geometries and ensure that the computational mesh is optimized to produce accurate and stable solutions (Gable et al., 1996a). Meshes can be classified as structured and unstructured, according to topological characteristics. The topology of a mesh defines how nodes are interconnected. Structured meshes are characterized by a foreseeable rule that describes node connectivity with neighboring nodes. On the contrary, unstructured meshes have no regular topology and the list neighbors must be stored for each node. In fact, there is no a repeatable pattern describing nodal connectivity, as relations between nodes change all over the domain. Unstructured meshes are the most general ones and they are broadly employed in geological models, especially in finite elements problems. An unstructured tetrahedral mesh is used here. A common algorithm to build a tetrahedral mesh is the extension to three dimensions of the Delaunay triangulation. A Delaunay triangulation for a set of nodes in a plane ensures that the circumcircle of any triangle contains no other input nodes. In three dimensions, triangles and circumcircles become tetrahedra and circumscribed spheres, respectively, such that every sphere must not contain nodes but the four tetrahedron's nodes.

[1] www.gocad.org
[2] http://www.geuz.org/gmsh/
[3] http://meshing.lanl.gov/

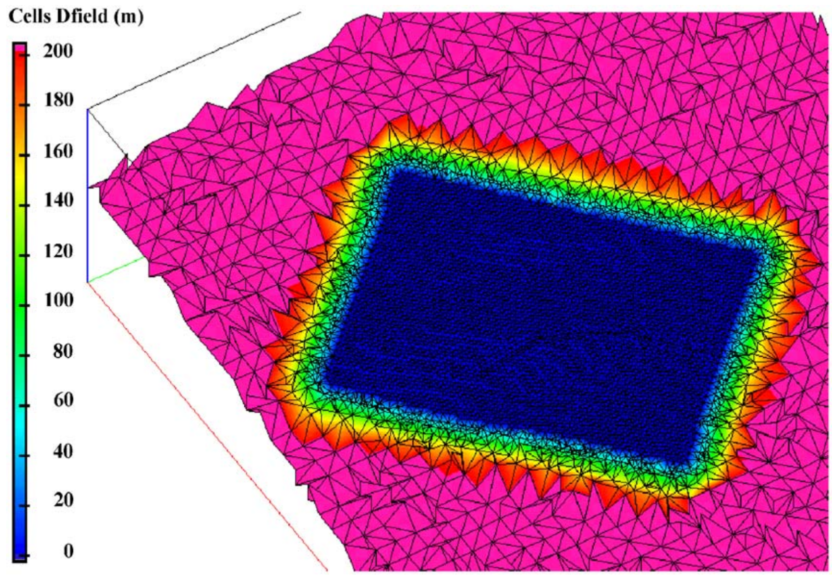

Fig. 1. Mesh refinement around a fracture: dfield cell attribute indicates distance from fracture.

The LaGriT mesh generation tool is based on the Delaunay algorithm and it guarantees that the fluid conductance matrix is a semi-positive definite matrix and ensures that flux calculations do not have negative transmissibilities (Gable et al., 1996b). Avoiding negative transmissibilities is necessary because they can lead to nonphysical simulated values, such as negative concentrations or saturations. LaGriT creates a mesh through three main steps: the geometric definition of surfaces and volumes, the distribution of nodes, and the connection of nodes into a mesh. The starting point for the coupling process between geological and numerical models is the application of the module of LaGriT capable of reading GOCAD TSurf files. Using this module, GOCAD surfaces are read as sheets, which are topologically 2D elements, but geometrically 3D objects constituted by a collection of connected triangles. Then, geometric regions are defined by logically combining surfaces coming from GOCAD and any other user-defined surface. The procedure developed to generate the mesh for a sample problem with few fractures zones uses the current LaGriT capabilities and it can be summarized by the following steps:

1. Import into LaGriT the GOCAD TSurf file for each fracture.
2. Create a hexahedral mesh covering the domain of interest. This mesh creates a distribution of nodes that will later be connected to form a tetrahedral mesh.
3. Refine the hexahedral elements that are close to the fractures.
4. Copy to a tetrahedral mesh object all nodes belonging to the hexahedral mesh and to the triangular meshes, representing the fractures, and connect those nodes using the Delaunay algorithm available in LaGriT.
5. Define two geometric regions around each fracture with the existing LaGriT operators, which are based on the notion of surface inward-pointing normal and surface outward-pointing normal. As a result, the 3D space containing the inward-pointing normal and the 3D space containing the outward-pointing normal are defined as two distinct regions separated by the fracture.
6. Extract a 2D triangulated surface from the 3D tetrahedral mesh. With this procedure, the interface between the two geometric regions defined at step 5 is extracted and used to obtain the final triangulated surface fracture (Fig. 1).

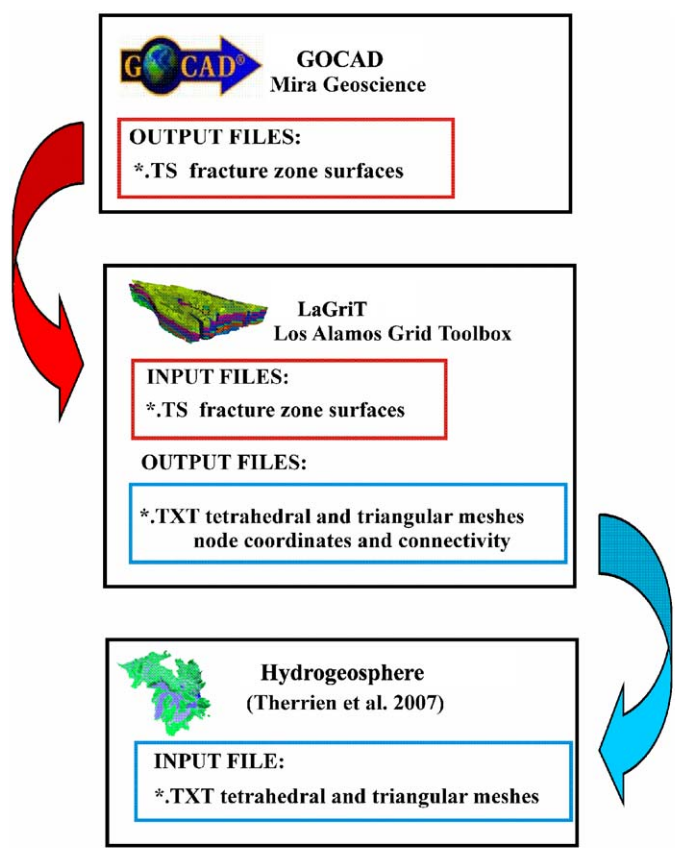

Fig. 2. Developed approach flowchart.

7. Output connectivity information for the tetrahedral and triangular meshes.

Once all seven steps are completed, the mesh information is read with the selected numerical code (see Section 3.1) and groundwater flow and contaminant transport can be simulated. A graphical view that summarizes the entire approach presented here is shown in Fig. 2.

3. Mathematical modeling

3.1. HydroGeoSphere

The numerical code selected here is HydroGeoSphere (Therrien et al., 2007). Listing all the features of HydroGeoSphere is beyond the scope of this paper and only those relevant to this work will be mentioned. HydroGeoSphere is a numerical simulator specifically developed for supporting water resource and engineering projects pertaining to hydrologic systems with surface and subsurface flow and contaminant transport components. It has been developed by Therrien et al. (2007), who extended the FRAC3DVS code to accommodate surface water flow and contaminant transport. The control-volume finite element method, CVFE, constitutes the basis for the numerical solution. Control-volume methods produce discretized equations by applying physical conservation laws to control-volumes surrounding mesh nodes. As a result, various terms in the discretized equations have a physically meaningful interpretation because the change in fluid mass storage for each volume is balanced by the term representing the divergence of the fluid mass flux in the same volume. Finite element methods, on the other hand, allow for the representation of complex geometrical domains with ease and efficiency. Thus, the CVFE method combines advantages from both techniques. The numerical implementation is presented in Therrien et al. (2007) and Therrien and Sudicky (1996) and will not be repeated, except for a few aspects linked to the approach proposed here.

The governing equation for 3D fully saturated groundwater flow in the porous matrix, without sources or sinks, is

$$\frac{\partial}{\partial x_i}\left(K\frac{\partial h}{\partial x_j}\right)=\frac{\partial S_s}{\partial t}\quad i,j=1,2,3 \tag{1}$$

and the 2D equation for fully saturated flow in discrete fractures is

$$\frac{\partial}{\partial x_i}(2b)\left(K_f\frac{\partial h}{\partial x_j}\right)=(2b)\frac{\partial S_{sf}}{\partial t}\quad i,j=1,2 \tag{2}$$

Contaminant transport in 3D porous media is described by

$$\frac{\partial c}{\partial t}+\frac{v_i}{R}\frac{\partial c}{\partial x_i}-\frac{\partial}{\partial x_i}\left(\frac{D_{ij}}{R}\frac{\partial c}{\partial x_j}\right)+\lambda c=0\quad i,j=1,2,3 \tag{3}$$

and the 2D transport equation in discrete fractures is

$$\frac{\partial c_f}{\partial t}+\frac{v_{f_i}}{R_f}\frac{\partial c_f}{\partial x_i}-\frac{\partial}{\partial x_i}\left(\frac{D_{f_{ij}}}{R_f}\frac{\partial c_f}{\partial x_j}\right)+\lambda c=0\quad i,j=1,2 \tag{4}$$

The standard Galerkin technique is used to discretize all the above equations (Therrien et al., 2007; Therrien and Sudicky, 1996). Using an approximation of the time derivative by a finite difference representation and a lumped mass approach to treat the storage terms, the discretized porous medium flow equation becomes

$$S_s\left(h_i^{t+1}-h_i^t\right)\frac{V_i}{\Delta t}=\sum_{\eta_i}\gamma_{ij}\left(h_j^{t+1}-h_i^{t+1}\right)\qquad i,j=1,2,3 \tag{5}$$

where parameter η_i is defined as being the set of nodes connected to node i and the term γ_{ij} contains the integral of the standard finite element basis functions that depend on the element type. The term γ_{ij} is sometimes referred to as the transmissibility (for example, Letniowski and Forsyth, 1991; Gable et al., 1996b), and Eq. (5) indicates that a negative transmissibility value will cause fluid flow from nodes with lower hydraulic heads towards nodes with higher hydraulic heads, which is physically unrealistic.

3.2. Numerical model development

In the HydroGeoSphere version described in Therrien et al. (2007), available elements to solve the 3D porous medium equations are either hexahedral blocks or triangular prisms (Fig. 3a), while in this work tetrahedral elements are proposed (Fig. 3b). With the discretely fractured medium representation, each fracture is explicitly represented by specifying its own geometry, areal extent, dimensions and position in the 3D space. The numerical approach is based on continuity of hydraulic head and concentration at the fracture/matrix interface, which corresponds to instantaneous equilibrium between the two domains. This method is also called the common node approach (Therrien et al., 2007; Therrien and Sudicky, 1996) and it is essentially based on superposition of 2D fracture elements onto the elements of the porous matrix (Fig. 4). Thus, nodes at fracture locations are common nodes that receive contributions from both the rock matrix elements and the fracture faces.

Representing irregular and non-planar fractures is more complex than representing regular fractures. The HydroGeoSphere code has been enhanced by Graf (2005) and Graf and Therrien (2008) to represent nonuniform inclined discrete fractures, adding the identification of internal faces in all 3D matrix elements (Fig. 4a). The work of Graf (2005) constitutes the basis for the development presented here and it is used to compare numerical results and verify the approach proposed in this paper. This approach is based on a new relationship, incorporated into the HydroGeoSphere model, between 2D triangular and 3D tetrahedral elements (Fig. 4b) representing, respectively, the fractures and the porous rock matrix. Compared to a regular mesh, a tetrahedral mesh allows local mesh refinement that does not propagate to the mesh boundaries. A tetrahedral mesh can also be adapted to complex geometrical domains, such as fractured media.

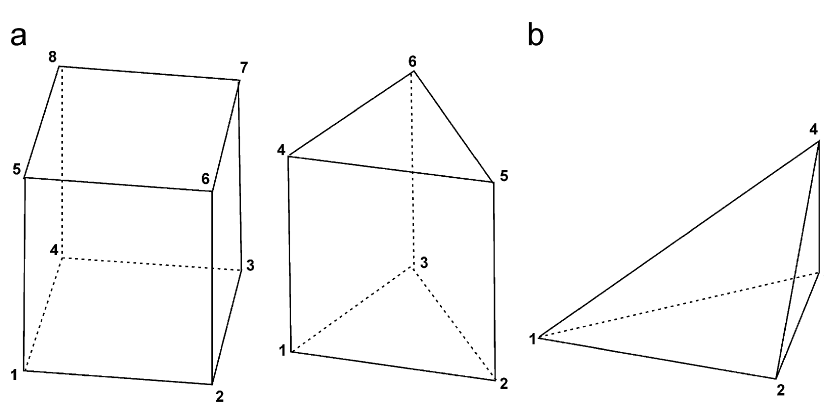

Fig. 3. Element types and local node numbering conventions: (a) HydroGeoShpere original version; (b) new element.

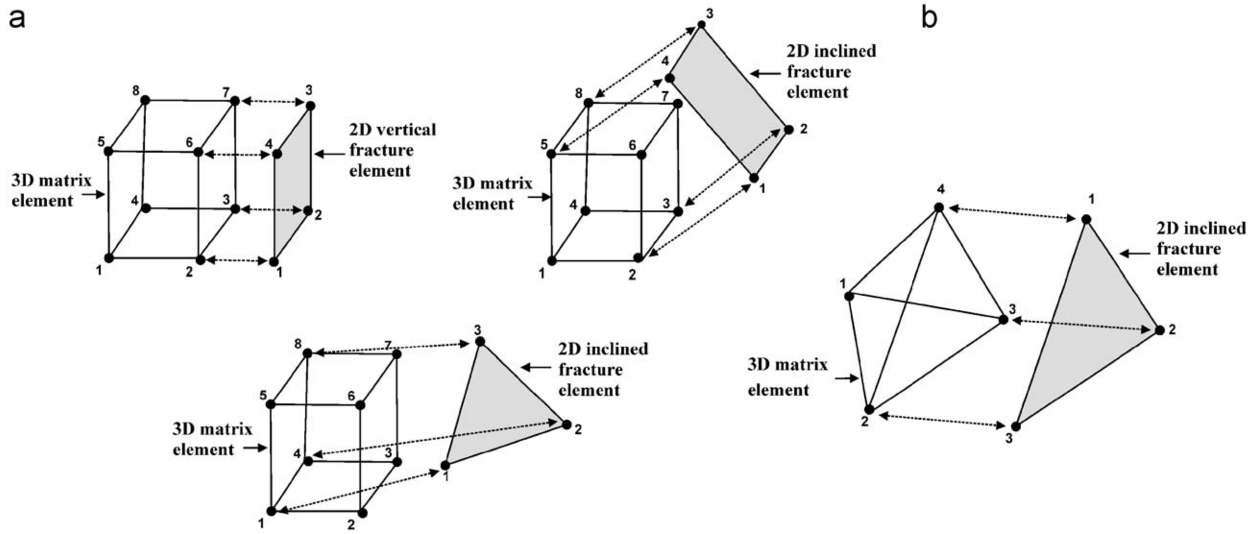

Fig. 4. Fracture elements representation: (a) HydroGeoSphere original version; (b) new representation.

To use both 2D triangles and 3D tetrahedra and to allow compatibility with the LaGriT software, modifications to the HydroGeoSphere code were required. For example, to compute mesh segments and faces, HydroGeoSphere uses the maximum number of segments connected to a single node. This number can be easily determined from geometry in structured and regular meshes and it is constant for block-based meshes. On the contrary, in tetrahedral meshes the maximum number of segments connected to a node may vary greatly depending on the complexity of the mesh. The mesh generator LaGriT provides this parameter and its value is incorporated into the HydroGeoSphere numerical code.

3.3. CVFE method and the fluid conductance matrix

The control-volume finite element method applied to numerical modeling in hydrogeology is discussed in Letniowski and Forsyth (1991). In this method, a finite volume subgrid is constructed as a complement to the finite element grid (Geiger et al., 2004). The CVFE method combines the flexibility of a finite element method with a local conservation property, which is typical of finite volume schemes. To evaluate the fluid conductance matrix, the influence coefficient technique proposed by Huyakorn et al. (1984) is used. The technique was first developed for linear rectangular elements and then applied to 3D blocks and prism elements (Huyakorn et al., 1986; Huyakorn et al., 1987; Beinhorn and Kolditz, 2003). It provides a rapid evaluation of fluid conductance matrix coefficients, without requiring numerical integration phases and therefore reducing computation effort (Huyakorn et al., 1984). The integral of the basis functions, represented by γ_{ij} in Eq. (5), is given by

$$\gamma_{ij} = \int_V \nabla N_i K \nabla N_j \, dV \tag{6}$$

and it can be directly replaced by the elemental influence coefficient matrix (Therrien and Sudicky, 1996). Coefficients γ_{ij} depend upon the type of elements and the shape functions chosen. Simplex tetrahedra have been chosen here. Simplex elements have linear sides and linear polynomials as interpolation function. For a tetrahedron whose vertices are i, j, k and l, the following known shape function is used (Allaire, 1985):

$$\{N\} = \frac{1}{6V}\{1, x, y, z\}\begin{bmatrix} a_i & a_j & a_k & a_l \\ b_i & b_j & b_k & b_l \\ c_i & c_j & c_k & c_l \\ d_i & d_j & d_k & d_l \end{bmatrix} \tag{7}$$

where V is the tetrahedron volume, calculated from the four nodes coordinates.

After evaluating the Jacobian matrix, or element derivative matrix, the elemental stiffness matrix can be calculated as

$$\begin{aligned} [A]^{(e)} &= K_{xx}\cdot[A_{xx}] + K_{yy}\cdot[A_{yy}] + K_{zz}\cdot[A_{zz}] \\ &= \frac{K_{xx}}{36V}\cdot\begin{bmatrix} b_ib_i & b_ib_j & b_ib_k & b_ib_l \\ & b_jb_j & b_jb_k & b_jb_l \\ & & b_kb_k & b_kb_l \\ & & & b_lb_l \end{bmatrix} \\ &+ \frac{K_{yy}}{36V}\cdot\begin{bmatrix} c_ic_i & c_ic_j & c_ic_k & c_ic_l \\ & c_jc_j & c_jc_k & c_jc_l \\ & & c_kc_k & c_kc_l \\ & & & c_lc_l \end{bmatrix} \\ &+ \frac{K_{zz}}{36V}\cdot\begin{bmatrix} d_id_i & d_id_j & d_id_k & d_id_l \\ & d_jd_j & d_jd_k & d_jd_l \\ & & d_kd_k & d_kd_l \\ & & & d_ld_l \end{bmatrix} \end{aligned} \tag{8}$$

In Eq. (8), matrices are symmetric and the half-lower matrices are omitted for the sake of clarity. Matrix A is called the stiffness matrix, even if this term usually refers to solid mechanics. For fluid mechanics, it might be more appropriate to call it the fluidity matrix or fluid conductance matrix as in Allaire (1985). The global matrix containing all elemental contributions is obtained after the assembly phase. This matrix may be an M-matrix, which is a real, square, nonsingular matrix A, whose off-diagonal elements γ_{ij} are either zero or negative and whose diagonal elements are strictly positive. The diagonal element γ_{ii} in the control-volume discretization is the sum of the absolute values of the other entries in row i, causing the matrix to be diagonally dominant. M-matrix properties can be summarized as follows (Kosik et al., 2000):

$$\begin{aligned} \gamma_{ij} &\leqslant 0 \quad \forall i \neq j \\ \gamma_{ii} &\geqslant -\sum_j \gamma_{ij} \quad \forall i \neq j \\ A^{-1} &\geqslant 0 \end{aligned} \tag{9}$$

Coefficients γ_{ij} of the fluid conductance matrix A are called transmissibilities (Letniowski and Forsyth, 1991; Letniowski, 1992) and their expression is given in Eq. (6). Transmissibility γ_{ij} can be evaluated analytically with Eq. (8), such that every γ_{ij} constitutes the entry (i,j) in the fluid conductance matrix A and corresponds to the tetrahedral edge of extremities i and j. Therefore, the flux between nodes i and j is given by

$$Q_{ij} = \gamma_{ij}(h_j - h_i) \tag{10}$$

An M-matrix is desirable for iterative sparse matrix solvers. The existence of an M-matrix implies that the so-called positive transmissibility (PT) condition is satisfied, which guarantees that the discrete flux between two nodes is in the opposite direction of the dependent variable gradient (Putti and Cordes, 1998). Otherwise, unrealistic results could be obtained, like a flux in the direction of increasing hydraulic heads. However, even in cases where the discrete solution does not demonstrate non-physical behavior, the violation of the PT condition may cause poor convergence behavior of the Newton iteration (Letniowski and Forsyth, 1991).

The Delaunay algorithm is commonly applied to discretize the space with triangles or tetrahedra. In two dimensions, the Delaunay algorithm ensures the generation of an M-matrix associated with the mesh (Cordes and Putti, 2001; Putti and Cordes, 1998). In the case of a constant permeability tensor, a given set of nodes in two dimensions can be triangulated such that all interior edges have positive transmissibilities. This is possible in two dimensions because of the equivalence of the positive transmissibility condition and a Delaunay triangulation (Letniowski and Forsyth, 1991). Kosik et al. (2000) came to the same conclusion, using the maximum principle in the solution of the diffusion equation. The violation of this principle can be detected by the emergence of negative concentrations and spurious oscillations, which are caused by negative transmissibilities, and the resulting nonphysical flows. Unfortunately, a 3D Delaunay triangulation does not, in general, produce positive transmissibilities. Of course, it is still possible to seek a triangulation that minimizes the number and size of the negative transmissibilities (Letniowski and Forsyth, 1991). Linear Galerkin finite element discretizations of the Laplace operator produce non-positive stiffness coefficients for internal element edges of two-dimensional Delaunay triangulations. This property is a prerequisite for the existence of an M-matrix and ensures that nonphysical local extrema are not present in the solution (Putti and Cordes, 1998). The Laplace operator of the partial differential equation is often discretized using the Galerkin method, but in the case of a 3D tetrahedral mesh it does not lead to an M-matrix. Therefore, it is interesting to analyze the orthogonal subdomain collocation (OSC) method proposed by Putti and Cordes (1998, 2000), which is based on a different interpretation of the standard Galerkin method. The OSC method considers as vertices of the control volumes the circumcenters and not the gravity centers of tetrahedra. The elemental stiffness coefficient can be obtained as the negative ratio between the area of the Voronoi cell face F_{ij} of the tetrahedron and the length of the corresponding element edge r_{ij} (Putti and Cordes, 1998)

$$\gamma_{ij}^{\mathrm{OSC}} = -\frac{F_{ij}}{|r_{ij}|} \tag{11}$$

For each tetrahedron, a $[4 \times 4]$ matrix is calculated. As a result, calculations are required only for six elements, whose expressions are derived from Eq. (11) with geometrical considerations. The expression for the first element γ_{ij} would be (see Cordes and Putti (2001) and Putti and Cordes (1998) for more details)

$$\gamma_{ij}^{e} = -\frac{1}{48V}\left[2(r_{ik}\,r_{jk})(r_{il}\,r_{jl}) + A_k A_l\left(\frac{(r_{ik}\,r_{jk})^2}{A_l A_l} + \frac{(r_{il}\,r_{jl})^2}{A_k A_k}\right)\right] \tag{12}$$

Transmissibilities are evaluated with Eq. (12) and an M-matrix is obtained. Therefore the OSC scheme preserves the physical correspondence between fluxes and gradients, avoiding unrealistic results.

4. Model verification

Test cases have been designed to verify the approach. First, the evaluation of the fluid conductance matrix for the tetrahedral mesh is verified (test cases 1A and 1B). Then, simulations of groundwater flow and transport for simple geometries show that the approach works properly (test cases 2, 3A, and 3B). Simulations are for steady state flow fields. Simulation results of tetrahedral mesh are shown for the Galerkin method. Moreover, a comparison between OSC and Galerkin methods is given for test case 3A by analyzing transport simulation results.

4.1. Test cases 1A and 1B: fluid conductance matrix

A first test has been carried out to verify the difference between the Galerkin and the orthogonal subdomain collocation methods to evaluate the elements of the fluid conductance matrix. In the test, a unit cubic node distribution has been used and six Delaunay tetrahedra (Fig. 5) have been created with LaGriT and then read by HydroGeoSphere. With the Galerkin method, the resulting global fluid conductance matrix has three off-diagonal entries that are positive (Fig. 6), violating the M-matrix definition. This demonstrates, as stated earlier, that in three dimensions a Delaunay tetrahedralization may not lead to an M-matrix (Cordes and Putti, 2001; Putti and Cordes, 1998; Letniowski, 1992; Letniowski and Forsyth, 1991). With the OSC approach (Cordes and Putti, 2001; Putti and Cordes, 1998), off-diagonal coefficients of the fluid conductance matrix (Fig. 7) are either zero or negative. Moreover, they are equal to those given by the LaGriT mesh generator, which guarantees that a Delaunay mesh produces an M-matrix.

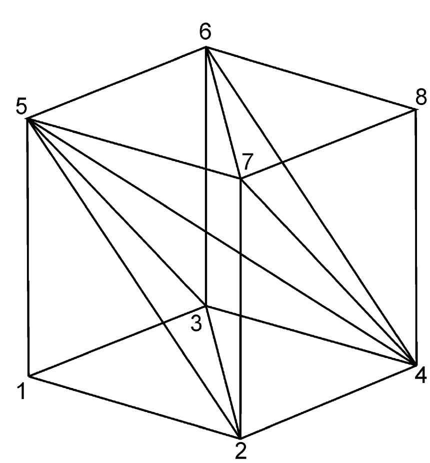

Fig. 5. Sample mesh: eight nodes, six tetrahedra.

$$\begin{bmatrix} 3/6 & -1/6 & -1/6 & 0 & -1/6 & 0 & 0 & 0 \\ & 5/6 & 1/6 & -3/6 & -1/6 & -1/6 & 0 & 0 \\ & & 5/6 & -3/6 & -1/6 & 0 & -1/6 & 0 \\ & & & 7/6 & 2/6 & -1/6 & -1/6 & -1/6 \\ & & & & 7/6 & -3/6 & -3/6 & 0 \\ & & & & & 5/6 & 1/6 & -1/6 \\ & & & & & & 5/6 & -1/6 \\ & & & & & & & 3/6 \end{bmatrix}$$

Fig. 6. Global matrix for eight nodes tetrahedral mesh: Galerkin method.

$$\begin{bmatrix} 3/4 & -1/4 & -1/4 & 0 & -1/4 & 0 & 0 & 0 \\ & 3/4 & 0 & -1/4 & 0 & -1/4 & 0 & 0 \\ & & 3/4 & -1/4 & 0 & 0 & -1/4 & 0 \\ & & & 3/4 & 0 & 0 & 0 & -1/4 \\ & & & & 3/4 & -1/4 & -1/4 & 0 \\ & & & & & 3/4 & 0 & -1/4 \\ & & & & & & 3/4 & -1/4 \\ & & & & & & & 3/4 \end{bmatrix}$$

Fig. 7. Global matrix for eight nodes tetrahedral mesh: OSC method.

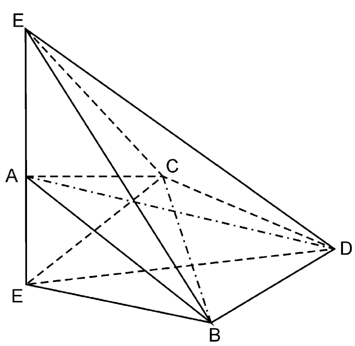

Fig. 8. Tetrahedral discretization used by Letniowski (1992).

Table 1
Transmissibility for segment AD.

Tetrahedron	γ_{AD} Galerkin method	γ_{AD} OSC method
ABDF	−0.0159	−0.007293
ACDF	−0.0050	0.011796
ABCD	2.2291	−0.007790
	$\gamma_{AD}{}^{G} = \gamma_{AD}{}^{ABDF} + \gamma_{AD}{}^{ACDF} + \gamma_{AD}{}^{ABCD}$	
GLOBAL $\gamma_{AD}{}^{G}$	2.2082	−0.003287

The enhanced code version capable of accommodating a tetrahedral mesh has been also verified with the example presented by Letniowski (1992), who considered a simple mesh composed of five tetrahedra (Fig. 8). The nodes have the spatial coordinates: $A=(-2,-2,0.5)$, $B=(0,-2,0.1)$, $C=(-2,0,0.1)$, $D=(0,0.1,0)$, $E=(-2,-2,-0.25)$, $F=(-2,-2,1.5)$. The mesh, created by Delaunay triangulation, contains five tetrahedra: ABDF, ACDF, ABCE, BCDE and ABCD. The standard Galerkin method is applied by Letniowski (1992) and the AD edge connection value equals 2.208 (Table 1). In comparison, the same coefficient calculated with the OSC method incorporated into HydroGeoSphere is equal to −0.0032872 (Table 1), which is the same value calculated by Putti and Cordes (1998), thus verifying the correct implementation of Eq. (12).

4.2. *Test case 2: groundwater flow and solute transport in a horizontal fracture*

The new modeling approach has been verified with an example previously solved with both an analytical method and finite block elements, to support the code development completed to date. In this example, the propagation of uranium, in its isotope form U^{234}, is simulated along a horizontal fracture embedded in a porous rock matrix. The horizontal fracture has been created in GOCAD and then imported into LaGriT. In this specific case, the fracture cuts through the whole domain (Fig. 9). A regular node distribution has been chosen, corresponding to block dimensions in the numerical example already treated in Therrien et al., (2007). The domain contains 410 nodes (respectively 41, 2 and 5 in the x, y, z directions), it has a unity thickness in the y-direction, a length of 200 m in the x-direction and a length of 0.1 m in the z-direction, such that elements orthogonal to the fracture have dimensions of 0.025 m. Simulation parameters are listed in Table 2. Observation points are placed along the fracture to visualize the concentration profile.

The same problem has been solved with the analytical solution CRAFLUSH (Sudicky, 1988), which solves the transport equation in

Table 2
Model parameters used in test case 2.

Parameter definition	Value
Source concentration at fracture origin, C_0 (kg/m^3)	1
Source concentration in the matrix (kg/m^3)	0
Velocity in the fracture (m/y)	100
Fracture aperture, $2b$ (m)	0.0001
Fracture spacing, B (m)	0.1
Longitudinal dispersivity in fracture, α_L (m)	1
Free solution diffusion coefficient, D_0 (m^2/y)	0.031536
Retardation factor in the matrix, R	14300
Tortuosity	0.1
Solute half-life, $T_{1/2}$ (y)	245000
Matrix porosity	0.01

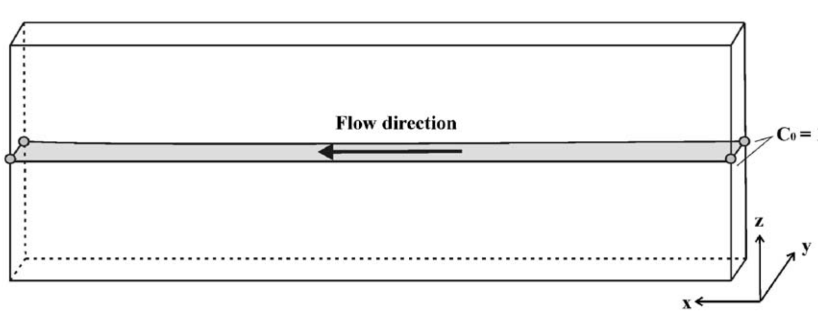

Fig. 9. Model design for test case 2: transport along a horizontal fracture.

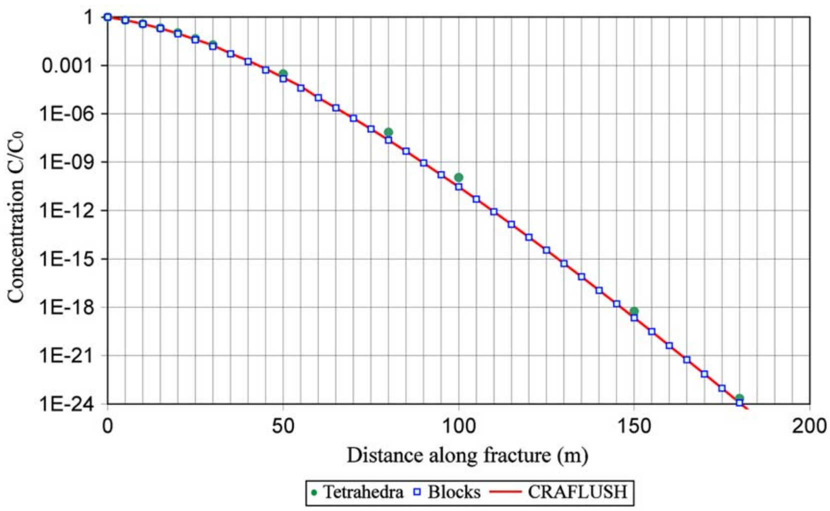

Fig. 10. Results test case 2: tetrahedral mesh, block-based mesh and analytical solution.

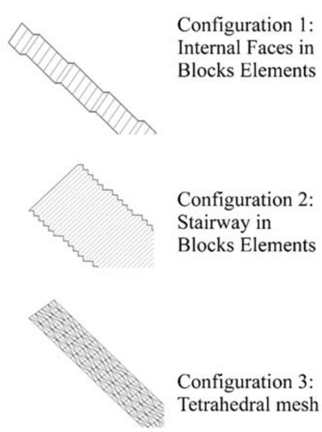

Fig. 11. Different fracture configurations.

a system of parallel fractures with matrix diffusion and longitudinal dispersion along the fracture. CRAFLUSH numerically inverts the Laplace transformed solution that is presented in the studies of Tang et al. (1981) and Sudicky and Frind (1982). The results obtained using HydroGeoSphere with the newly implemented tetrahedral mesh agree very well with the analytical solution results (Fig. 10). The comparison with a block-based mesh shows two very similar concentration profiles because the fracture is horizontal and the use of blocks or tetrahedra does not affect the geometry of the discretized fracture.

4.3. Test cases 3A and 3B: transport in a single inclined fracture

For test case 3A, two different discretized fracture configurations based on a block-based mesh (Fig. 11, configurations 1 and 2) are compared to the new representation based on the tetrahedral mesh (Fig. 11, configuration 3). The block-based mesh contains 24,442 nodes and 12,000 elements. It is 10 m and 12 m long in the vertical direction and horizontal directions, respectively, with a unit thickness in the third direction. The tetrahedral mesh has been generated from a regular node distribution with 61 nodes along the x-axis, 51 along the z-axis and 2 along the y-axis. The mesh was then refined around the inclined fracture. The refined mesh (Fig. 12) has 3609 nodes and 14,279 tetrahedra. The block-based and tetrahedral mesh simulations both consider a constant

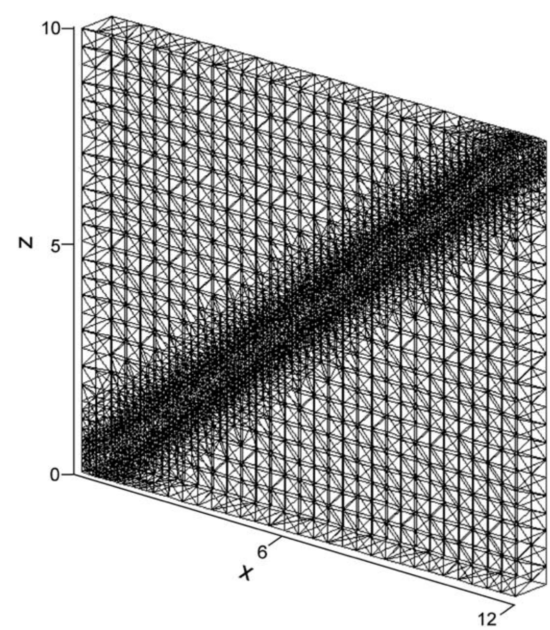

Fig. 12. Tetrahedral mesh with refinement around an inclined fracture for case 3A.

concentration of contaminant equal to 1.0 on the top of the domain (Fig. 13). All other boundaries are assigned zero dispersive flux for transport. An inclined fracture (about 40°) crosses the whole domain. Specified head conditions are imposed at $x=0$ and $x=12$, with a hydraulic head difference equal to 0.5 m. Other simulation parameters are listed in Table 3. An observation point is located at coordinates (6,0,5). The fracture strongly controls the solute migration and different fracture configurations provide comparable breakthrough curves (Fig. 14). However, the tetrahedral mesh gives a result closer to the Blocks_Internal_Faces curve than to the Block_Stairway curve, as may be expected since the fracture in the tetrahedral mesh is like a sheet and the solute pathway is not lengthened, which is the case for the block-stairway configuration. Computed concentrations indicate that the minimum value obtained with the OSC method is exactly 0, which is equal to the initial concentration imposed in the domain. In contrast, a negative value of -3.6×10^{-4} is obtained with the Galerkin method. Negative concentration values, even if they are small in this case, are clearly nonphysical since they correspond to a negative mass. Therefore, the OSC method seems to be more appropriate than Galerkin method, especially for transport simulations.

Another simulation, test case 3B, was run to verify the fracture behavior. The geometry is the same as used previously, but now heads and concentration are only imposed at the extremities of the fracture (Fig. 13). Simulation parameters are listed in Table 3. The surrounding rock matrix is considered impermeable, such that the solute propagation along the fracture could be evaluated with the simplified Ogata–Banks analytical solution applicable when the observation point is far from the source of solute, and which expresses concentration as

$$c(x,t) = \frac{c_0}{2}\,\mathrm{erfc}\left(\frac{x - \nu t}{2\sqrt{Dt}}\right) \tag{13}$$

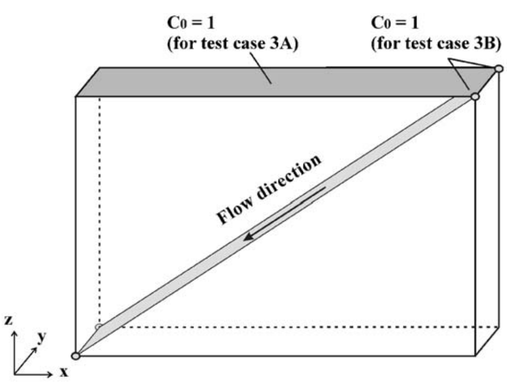

Fig. 13. Model design for test cases 3A and 3B: transport along a single inclined fracture.

Table 3
Model parameters used in test cases 3A and 3B.

Parameter definition	Value
Source concentration, C_0 (kg/m^3)	1
Fracture aperture, $2b$ (m)	0.0002
Longitudinal dispersivity in fracture, α_L (m)	0.1
Free solution diffusion coefficient, D_0 (m^2/y)	0.15768
Tortuosity, τ	0.1
Matrix porosity	0.35
Matrix hydraulic conductivity (m/y)	0.864
Matrix longitudinal dispersivity, α_L (m)	0.1

The velocity along the fracture is 0.00093 m/s. Simulation results are shown in Fig. 15. The solute breakthrough curves computed at the observation point show that the tetrahedral mesh gives a very good approximation of the Ogata–Banks analytical solution, even better than the Blocks_Internal_Faces solution. The Blocks_Stairway configuration is obviously the worst one, as the travel distance is lengthened compared to a planar fracture. Thus, the mesh generation process adopted here leads to a better representation of inclined fractures.

5. Summary and conclusion

A new modeling approach for fractured geological media is presented here. It is based on the combination of the geological modeling platform GOCAD, the mesh generation software LaGriT and the numerical model HydroGeoSphere. Fractures are built in the geological modeling platform and they are represented by conforming triangulated surfaces, such that they can be easily visualized and their geometry modified before the 3D mesh is generated. The 3D tetrahedral mesh is created with LaGriT and it is easily refined around fractures. The enhanced HydroGeoSphere version can read 3D tetrahedral mesh data in LaGriT format and some tetrahedral faces are then selected and defined as 2D triangular fracture elements.

Several test cases are carried out to verify the approach proposed. First, the evaluation of coefficients in the fluid conductance matrix for the tetrahedral unstructured mesh is verified. Moreover, an application of the orthogonal subdomain collocation method shows how an M-matrix can be obtained with a Delaunay tetrahedral mesh. Then, simulation results obtained with the new mesh configuration proposed are compared with a known analytical solution and with other numerical results. A good match exists with the analytical solution presented. Furthermore, comparison with block-based meshes proves that the approach presented in this paper offers a better way to represent discretized fractures, without increasing their path length. In conclusion, the fracture configuration proposed here, which is based on the combination of tetrahedral and triangular finite elements, is shown to be appropriate and the application of the whole modeling approach is straightforward. This paper focuses on the verification of the correct implementation of the proposed approach, which is based on the coupling of different modeling tools. Simple test cases are presented as the first application of the approach. Future work will extend the application of the approach to more complex domains, which

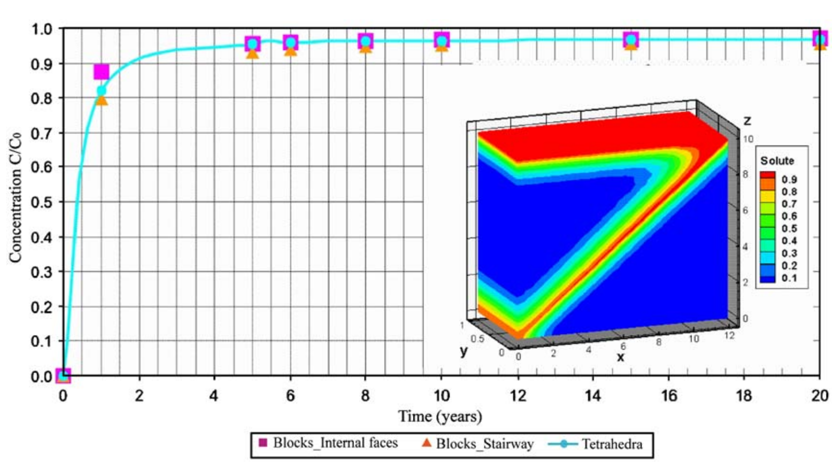

Fig. 14. Results test case 3A: tetrahedral mesh and block-based mesh.

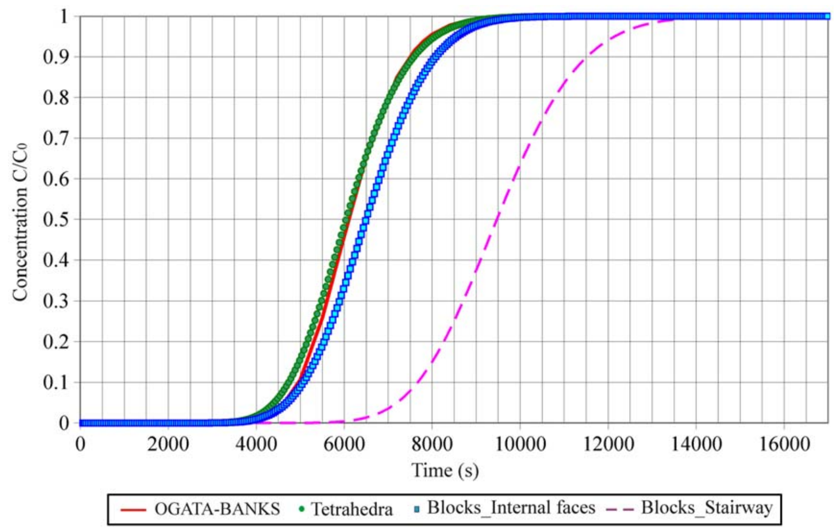

Fig. 15. Results test case 3B: tetrahedral mesh, block-based mesh and analytical solution.

can include intersecting fractures and pumping wells. An application to a real site will show the applicability and utility of the modeling approach presented here.

Acknowledgements

This work was supported by the GEOIDE network through the Networks of Centres of Excellence program of the Canadian government. The first author thanks C.W. Gable (Los Alamos National Laboratory) for his help with the LaGriT software. The constructive comments of two anonymous reviewers are greatly appreciated and have helped improve the manuscript.

References

Andenmatten-Berthoud, N., Kohl, T., 2003. Assessment and evaluation of geothermal potential in Switzerland (Atlas des ressources géothermiques suisses). Publication 230308, Commission Suisse de Géophysique, Zurich, Switzerland, 58p.

Allaire, P.E., 1985. Basis of the Finite Element Method Solid Mechanics Heat Transfer and Fluid Mechanics. Wm. C. Brown Publishers, Dubuque, IA, 691p.

Beinhorn, M., Kolditz, O., 2003. Triangular prismatic elements part II: analytical integration, GeoSys-Preprint. Technical Report no. 2003-30, Center for Applied Geosciences, University of Tübingen, Tübingen, Germany, 24pp.

Bower, K.M., Gable, C.W., Zyvoloski, G.A., 2005. Grid resolution study of ground water flow and transport. Ground Water 43 (1), 122–132.

Cordes, C., Putti, M., 2001. Accuracy of Galerkin finite-element for groundwater flow simulations in two and three dimensional triangulations. International Journal for Numerical Methods in Engineering 52 (4), 371–387.

Gable, C.W., Trease, H.E., Cherry, T.A., 1996a. Automated grid generation from models of complex geologic structure and stratigraphy. In: Proceedings of the Third International Conference/Workshop on Integrating GIS and Environmental Modeling, Santa Fe, NM, 10p.

Gable, C.W., Trease, H.E., Cherry, T.A., 1996b. Geological applications of automatic grid generation tools for finite elements applied to porous flow modeling. In: Soni, B.K., Thompson, J.F., Hausser, H., Eiseman, P.R. (Eds.), Proceedings of the Fifth International Conference on Numerical Grid Generation in Computational Fluid Dynamics and Related Fields. Mississippi State University, MS, p. 9.

Geiger, S., Roberts, S., Matthai, S.K., Zoppou, C., Burri, A., 2004. Combining finite element and finite volume methods for efficient multiphase flow simulations in highly heterogeneous and structurally complex geologic media. Geofluids 4 (4), 284–299.

Graf, T., 2005. Modeling coupled thermohaline flow and reactive solute transport in discretely-fractured porous media. PhD Dissertation, Université Laval, Québec City, Canada, 209p.

Graf, T., Therrien, R., 2008. A method to discretize non-planar fractures for 3D subsurface flow and transport simulations. International Journal for Numerical Methods in Fluids 56 (11), 2069–2090.

Huyakorn, P.S., Andersen, P.F., Mercer, J.W., White, H.O., 1987. Saltwater intrusion in aquifers: development and testing of a three-dimensional finite-element model. Water Resources Research 23 (2), 293–312.

Huyakorn, P.S., Springer, E.P., Guvanasen, V., Wadsworth, T.D., 1986. A three-dimensional finite-element model for simulating water flow in variably saturated porous media. Water Resources Research 22 (13), 1790–1808.

Huyakorn, P.S., Thomas, S.D., Thompson, B.M., 1984. Techniques for making finite-element competitive in modeling flow in variably saturated porous media. Water Resources Research 20 (8), 1099–1115.

Kalbacher, T., Wang, W., McDermott, C., Kolditz, O., Taniguchi, T., 2005. Development and application of a CAD interface for fractured rock. Environmental Geology 47 (7), 1017–1027.

Kolditz, O., Bauer, S., 2004. A process-orientated approach to compute multifield problems in porous medium. Journal of Hydroinformatics 6 (3), 225–244.

Kolditz, O., Delfs, J.O., Burger, C.M., Beinhorn, M., Park, C-H., 2008. Numerical analysis of coupled hydrosystems based on an object-oriented compartment approach. Journal of Hydroinformatics 10 (3), 227–244.

Kosik, R., Fleischmann, P., Haindl, B., Pietra, P., Selberherr, S., 2000. On the interplay between meshing and discretization in three-dimensional diffusion simulation. IEEE Transactions on Computer-Aided Design of Integrated Circuits and Systems 19 (11), 1233–1240.

Letniowski, F.W., 1992. Three-dimensional Delaunay triangulations for finite-element approximations to a second-order diffusion operator. SIAM Journal on Scientific and Statistical Computing 13 (3), 765–770.

Letniowski, F.W., Forsyth, P.A., 1991. A control volume finite-element method for three dimensional NAPL groundwater contamination. International Journal for Numerical Methods in Fluids 13 (8), 955–970.

Mallet, J.-L., 2002. Geomodeling. Oxford University Press, New York, NY, 599p.

Putti, M., Cordes, C., 1998. Finite-element approximation of the diffusion operator on tetrahedra. SIAM Journal on Scientific Computing 19 (4), 1154–1168.

Sudicky, E.A., 1988. CRAFLUSH, Programmer's Guide. Waterloo Centre for Groundwater Research, University of Waterloo, Waterloo, Ontario, Canada, 12p.

Sudicky, E.A., Frind, E.O., 1982. Contaminant transport in fractured porous media: analytical solutions for a system of parallel fractures. Water Resources Research 18 (6), 1634–1642.

Tang, D.H., Frind, E.O., Sudicky, E.A., 1981. Contaminant transport in fractured porous media: analytical solution for a single fracture. Water Resources Research 17 (3), 555–564.

Taniguchi, T., Fillion, E., 1996. Numerical experiments for 3-dimensional flow analysis in a fractured rock with porous matrix. Advances in Water Resources 19 (2), 97–107.

Therrien, R., McLaren, R.G., Sudicky, E.A., Panday, S.M., 2007. HydroGeoSphere—A Three-Dimensional Numerical Model Describing Fully-Integrated Subsurface and Surface Flow and Solute Transport. Users's Guide. Université Laval and University of Waterloo, Canada, 379p.

Therrien, R., Sudicky, E.A., 1996. Three-dimensional analysis of variably saturated flow and solute transport in discretely-fractured porous media. Journal of Contaminant Hydrology 23 (6), 1–44.